Phys. Scr. **T155** (2013) 014005 (8pp) doi:10.1088/0031-8949/2013/T155/014005

Cylindric filaments and velocity structure functions

V A Sirota and K P Zybin

P N Lebedev Physical Institute of RAS, 119991, Leninskij pr. 53, Moscow, Russia

E-mail: sirota@lpi.ru and zybin@lpi.ru

Received 28 April 2012
Accepted for publication 12 May 2012
Published 16 July 2013
Online at stacks.iop.org/PhysScr/T155/014005

Abstract
We analyze a particular simple case within the framework of the vortex filament (VF) model. It gives the same basic results and allows us to understand the general case better. Advantages and weaknesses of the simplification are considered. The introduction of stochastics into the Navier–Stokes equation, the evolution of VFs and longitudinal and transverse Euler velocity structure functions are analyzed in terms of cylindric filaments.

PACS numbers: 47.10.ad, 47.27.De, 47.27.eb, 47.27.Gs

1. Introduction

One of the fundamental problems in turbulence is the determination of correlators, in particular, velocity structure functions. These functions are believed to be power laws inside the inertial range of scales, i.e. the range where scales are much less than the largest eddy scale, and viscosity is negligible. The canonical consideration implies that the scaling exponents are independent of (or at least depend very weakly on) the details of the flow, in particular, on the Reynolds number.

Experiments and direct numerical simulations (DNS) of hydrodynamical turbulent flow seem to have overtaken theoretical investigations in this direction. Numerous DNS, as well as high-resolution experiments performed during the last 20 years [1], allowed us to measure the first ten scaling exponents with high accuracy. The exponents show strongly intermittent behavior, i.e. the dependence on n is nonlinear. The new result observed in the DNS [2–4] and experiments [5, 6] is the difference between longitudinal and transverse scaling exponents, even though the flow is isotropic.

The multifractal (MF) model [7, 8] is a successful framework for describing and interpreting the observed intermittency. But this model is based on dimensional considerations, and the function $D(h)$ used to derive the scaling exponents is itself to be explained by means of the Navier–Stokes equation (NSE).

The vortex filament (VF) model [9–14] emerged as an attempt to find a physical explanation for the observed intermittency. It was based on the NSE and succeeded in deriving the correct scaling exponents, but still lacked simple and plain formulations. It appears that many of the results of the VF theory can be understood by consideration of a simple cylindrical model of VFs [14, 15]. Moreover, the simple example allows us to formulate some statements in a more exact way than in the general case. However, this simplification implies of course some additional difficulties. In this paper, we comment on the VF model and derive some of its results on the basis of the particular case of a cylindrical VF.

We consider fully developed turbulence in an incompressible liquid. Since we are interested in the properties of the inertial range, we neglect the effects of viscosity. However, we consider only those solutions to the Euler equation that can be obtained as the limit of a sequence of 'viscous' solutions. (In a sense, we consider the inviscid limit of the NSE.)

In section 2, we introduce the cylindrical VF. We define the locally homogeneous large-scale flow that can be produced by forces acting, e.g., on a sphere of some large radius. Then we add small-scale fluctuations and show that the evolution of vorticity is determined in the model by the large-scale force. We also discuss the relation to two-dimensional (2D) turbulence. This allows us to check the existence of the solutions. In section 2.4, we discuss the dynamical evolution of the described system.

In section 3, we discuss possible ways of introducing stochasticity into the NSE. We show that the way this is done in the VF model corresponds to introducing random boundary conditions into the NSE, instead of external large-scale random forces. Then we briefly recall the derivation of statistic moments of the vorticity and the asymptotic vorticity probability density function (PDF) obtained in previous papers, and comment on the availability of the model.

In section 4, following [15, 16], we combine the cylindrical model with the MF model to calculate longitudinal and transverse structure functions. Extreme filaments that make a major contribution to the scaling exponents of very high order are discussed in detail. It is shown that transverse scaling exponents are well described by the cylindrical model, while for longitudinal scaling exponents of high order one has to take strongly curved filaments into account.

2. Cylindrical model: dynamics

The main idea of the VF model is that regions of high vorticity (VFs) are responsible for the observed intermittent properties of a turbulent flow. Fast rotations stabilize the motion inside the filament and provide the conditions for exponential growth of vorticity.

Here, we consider a simplified model that we hope to reveal the main properties of VFs. In this model, all VFs are straight, and are aligned with the same axis, so we do not need to bother about their curvature for some time. This straightening is achieved by choosing special boundary conditions for the Euler equation, which in turn corresponds to a special form of large-scale perturbations.

2.1. Large-scale flow

Let an axially symmetric large-scale flow inside some sphere of a large radius R be described by the relations

$$v_\rho = a(t)\rho, \quad v_z = b(t)z. \tag{1}$$

Here ρ, z are the radial and the axial cylindrical coordinates, respectively. The flow is homogeneous: shifting of the origin of the coordinates to any co-moving point would not change the local construction of the flow. It is also evident that the vorticity of the flow is zero.

To satisfy the Euler equation, the pressure must take the form

$$p = \tfrac{1}{2}p_1(t)\rho^2 + \tfrac{1}{2}p_2(t)z^2.$$

From the incompressibility condition and the Euler equation we obtain

$$2a + b = 0, \quad \dot{a} + a^2 = -p_1, \quad \dot{b} + b^2 = -p_2. \tag{2}$$

There are three equations and four functions, so the value $p_2(t)$ can be treated as a boundary condition. It governs the changes in the flow along the z-axis, while $p_1(t)$ keeps the balance of forces across the cylinder.

The flow (1) can be produced by large-scale surface forces acting on a sphere of a large radius R. Then the value $p_2(t)$ may be interpreted as the large-scale surface force. The solution outside the sphere R would then decay at large distance.

Actually, in spherical coordinates, (1) can be written as

$$v_r = ar(1-3\mu^2), \quad v_\theta = 3ar\sin\theta\cos\theta,$$
$$v_\phi = 0, \quad \mu = \cos\theta.$$

The condition of zero divergence allows us to introduce the stream function $\psi(r,\theta)$ such that

$$v_\theta = \frac{1}{r\sin\theta}\frac{\partial\psi}{\partial r}, \quad v_r = -\frac{1}{r^2\sin\theta}\frac{\partial\psi}{\partial\theta}.$$

Integrating the solution inside the sphere R, we obtain

$$\psi = ar^3(\mu - \mu^3), \quad r < R.$$

The condition for the stream function outside the sphere ($r > R$) comes from the requirement of zero vorticity. The axial and radial components of vorticity are automatically zero since the solution does not depend on the axial variable; the third component is

$$\omega_\phi = \frac{1}{r}\frac{\partial}{\partial r}(rv_\theta) - \frac{1}{r}\frac{\partial}{\partial\theta}v_r.$$

Substituting the definition of ψ, we obtain

$$r^2\psi_{rr} + (1-\mu^2)\psi_{\mu\mu} = 0.$$

The decaying solutions of this equation satisfy $\partial\psi/\partial\mu = \sum C_l r^{-l} P_l(\mu)$, where $P_l(\mu)$ is the Legendre polynomial. Matching this with the solution in the inner zone, we find that only $l = 2$ is appropriate; thus, in the outer zone we obtain

$$\psi = a(t)\frac{R^5}{r^2}\left(\mu - \mu^3\right), \quad r > R. \tag{3}$$

Taking the derivatives, one can now obtain the velocities at $r > R$.

Thus, the large-scale flow (1), (3) can be thought of as a flow in an infinite volume with large-scale forces acting on the sphere of radius R.

The solution inside the sphere is uniquely determined by the initial and boundary conditions: indeed, since the initial vorticity inside the sphere is zero, and the boundary forces have no rotational moment, the flow remains irrotational. So, velocity can be written as $\mathbf{v} = \nabla\Phi$ and, because of zero divergence, $\Delta\Phi = 0$. Now, the boundary conditions are chosen to be quadrupole, so the only freedom degree for the solution is the function $b(t)$ restricted by (2).

We note that $p_2(t)$ is not arbitrary. Actually, for some $p_2(t)$ (for instance, constant and negative), the solution of (2) may become infinite at some finite time. However, this is forbidden by the physical meaning of the process. So, the choice of $p_2(t)$ must not allow infinite a (and, hence, infinite velocities). For 'real' forces acting at radius R this condition would hold automatically. We will return to this comment later on, when the formation of filaments will be described.

2.2. Small-scale pulsations

As we have introduced cylindrical large-scale flow, we now introduce small-scale perturbations. Since we wish to investigate 'straightened' filaments, we also put corresponding restrictions on these perturbations in order to keep the picture 'cylindrical'.

So, let the velocity distribution now take the form

$$\mathbf{v}(\mathbf{r}, t) = \mathbf{e}_z b(t)z + \mathbf{e}_r a(t)r + \mathbf{u}.$$

Here **u** is a velocity field orthogonal to the z-axis, and independent of z variable. It contains all the vorticity $\boldsymbol{\omega}$ of the flow (ω is directed along the z-axis). From the incompressibility of the flow it follows that $\nabla \cdot u = 0$. We must also add an additional component $\tilde{p}$ to the pressure; evidently, it does not depend on z. The NSE takes the form

$$\frac{\mathrm{d}\mathbf{u}}{\mathrm{d}t} + a\mathbf{u} + \nabla\tilde{p} = 0, \tag{4}$$

where $\mathrm{d}/\mathrm{d}t$ is the derivative along the particle trajectory. The velocity field $\mathbf{u}(t)$ is now restricted only by the condition that $\nabla\tilde{p}$ is conservative, i.e. that $\nabla \times (\nabla\tilde{p}) = 0$. Taking the curl of (4) and keeping in mind (2), we rewrite the condition in the form

$$\frac{\mathrm{d}\omega}{\mathrm{d}t} - b\omega = 0. \tag{5}$$

Taking one more time derivative and substituting $\dot{b}$ from (2) gives

$$\frac{\mathrm{d}^2\omega}{\mathrm{d}t^2} = p_2(t)\omega. \tag{6}$$

We find that, no matter what the initial velocity field is, the evolution of vorticity along a particle's trajectory is determined by the 'external' large-scale force p_2, which in our model is independent of **u**!

In the general case, an equation analogous to (6) can be written to describe the evolution of the vorticity vector: $\mathrm{d}^2\omega_i/\mathrm{d}t^2 = \rho_{ij}(t)\omega_j$. This equation is an exact consequence of the NSE, without any additional assumptions. The value p_2 corresponds here to the component of ρ_{ij} that is 'parallel' to vorticity, i.e. $\rho_{ij}\omega_i\omega_j/\omega^2$. The main hypothesis of the VF theory is that, in general filaments, this component also corresponds to a large-scale force and is independent of local vorticity.

2.3. Relation to 2D turbulence

We stress that the flow we have described here is *not* 2D. The essential point is that there is (large-scale) motion along the z-axis, which would provide stretching of a filament in the z-direction and compression in orthogonal directions.

However, there exists a correspondence between the solutions **u** to equation (4) and the solutions to the two-dimensional NSE. To find this correspondence, we rewrite (4) in Cartesian coordinates, and add viscosity to the right-hand side:

$$\frac{\partial}{\partial t}u_i + a(\rho_k\nabla_k)u_i + (u_k\nabla_k)u_i + au_i + \nabla_i\tilde{p} = \nu\Delta u_i.$$

Let $Q(t)$ be some function that satisfies the equation $\dot{Q} = a(t)Q$. We introduce new variables:

$$X_1 = x/Q(t), \quad X_2 = y/Q(t), \quad \mathbf{w} = Q(t)\mathbf{u},$$
$$\tau = \int \mathrm{d}t/Q^2(t), \quad \tilde{\tilde{p}} = Q^2\tilde{p}.$$

The equation then takes the form

$$\frac{\partial}{\partial t}w_i + w_k\frac{\partial}{\partial X_k}w_i + \frac{\partial}{\partial X_i}\tilde{\tilde{p}} = \nu\frac{\partial^2}{\partial X_i}w_i,$$

which coincides with the 2D NSE.

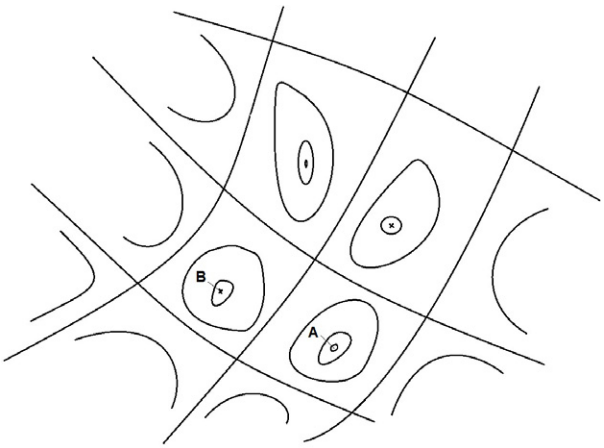

Figure 1. Isolines of vorticity. Separatrices correspond to $\omega = 0$. The points A and B are the centers of velocity filaments with opposite directions of vorticity.

Thus, any solution $\mathbf{u}(\rho, t)$ to equation (4) corresponds to some 2D solution. In the 2D case, the solution exists and is unique for a general 2D domain [17]. Hence, the same is true for (4). The only condition is $Q(t) \neq 0$ for any t, which corresponds to the requirement of finite $a(t)$.

2.4. Evolution of a filament

The vorticity evolution along any of the particle trajectories is determined by the large-scale value $p_2(t)$, and is described by equation (6). Different trajectories imply different initial conditions. Now we analyze possible solutions to the equation and therefore possible ways of evolution of the flow.

In the simplest case $p_2(t) = \mathrm{const}$, the answer is evident if $p_2 > 0$, vorticity grows (or decreases) exponentially: if $p_2 < 0$, the solution oscillates. In the case of arbitrary $p_2(t)$, one can obtain an approximate impression of the solution as a combination of exponential and oscillating sections.

We now note recall that, because of (5), the finiteness of $b = -2a$ requires that $\dot{\omega} = 0$ if $\omega = 0$. So, if vorticity is zero at some initial point, it must be zero along the whole trajectory. Also, the sign of vorticity cannot change along a particle's trajectory. Thus, if the initial ω is positive, the 'oscillating' parts must be short enough to not make it negative. So, for the evolution of vorticity along the particle trajectories, there are three possibilities: it varies near some value (p_2 changes its sign) or it decreases slowly to zero (p_2 is positive most of the time; special phases pick out the decreasing branch) or it increases exponentially (p_2 is positive most of the time). In what follows, we will be interested in the last case; we will show that it makes a major contribution to the statistics.

The prohibition of oscillations is a shortcoming of the cylindrical model. It is retribution for reducing vorticity to one dimension. In the general 3D case, b is a tensor, and each component of vorticity may change its sign. However, in what follows, we will need mostly the functions $p_2(t)$ that are positive, large and nearly constant, so this difference between the cylindrical model and the general case is not crucial.

Figure 1 presents a general view of the lines of constant vorticity in a plane orthogonal to $\mathbf{e}_z$ ('vorticity map'). The points A and B correspond to local maximums of the vorticity module, one with positive vorticity and another

with negative vorticity. The whole plane is generally divided into 'cells' separated by isolines of zero vorticity. Because of the large-scale flow, the particles move along the z-axis, so the evolution along the particle's trajectory corresponds, roughly speaking, to the dependence on z, and one can discuss the time evolution of the whole (x, y)-plane. (We note that the large-scale flow is locally homogeneous, so it acts equivalently in all cells.) Since the sign of vorticity cannot change along a trajectory, we see that each cell evolves separately, and different cells do not mix. In this sense, the topology of the flow does not change.

As we have seen from the analysis of (6), if $p_2(t)$ is positive most of the time, vorticity in some cells (cylinders) would increase exponentially as a function of time (at least, on average). We call these cells VFs. The independence of different cells implies that the neighborhood does not affect a filament. In particular, two filaments do not disturb each other significantly even when the distance between them is small.

Two VFs with opposite signs of vorticity can be closed and form a ring with two turning points on the sphere where large-scale forces are located. Our cylindric model does not allow linking of vortex lines.

3. Statistical description

3.1. Introduction of statistics

Introduction of stochasticity into the Navier–Stokes is usually done by adding some random large-scale forces acting on the entire liquid volume. It is assumed that, being large scale, these forces do not distort the flow at the scales inside the inertial range, but only pump the energy, providing the energy flux from larger to smaller scales. However, in real physical systems there are usually no volume external forces. A more 'realistic' problem statement would imply stochastic boundary conditions; but in such a formulation, a problem becomes difficult to solve. The approach we propose in the VF model allows us to reformulate stochastic boundary conditions as a stochastic coefficient in the equation that describes vorticity evolution along a particle's trajectory. Actually, equation (6) (or its 3D analogue) contains a large-scale value $p_2(x)$ that has the meaning of a force acting at the boundary of the flow.

Thus, we consider equation (6) (or, in the general case, its 3D analogue) instead of the NSE and suggest that $p_2(t)$ is a random process. Since p_2 is large scale, we assume it to be independent of local vorticity.

Since we now treat $p_2(t)$ as a random process, we need an ensemble of realizations of the large-scale flow (1). In each realization, the evolution of the small-scale flow is described by equation (6) with some definite $p_2(t)$. The statistical properties of a flow can be obtained by averaging over all possible realizations.

3.2. Correlators of vorticity

For simplicity, we first assume that $p_2(t)$ is Gaussian and delta-correlated, and then generalize the consideration.

Calculation of vorticity correlators based on the 1D equation (6), as well as the corresponding 3D general equation, was performed in [10, 11, 14]. Here we recall the results and comment on them from the point of view of the cylindrical model.

Consider equation (6) again, and rewrite it as a set of two first-order equations:

$$\dot{\omega} = v, \quad \dot{v} = p_2\omega.$$

Let p_2 be a stationary Gaussian random function. Supposing delta-correlation of p_2 and integrating (6) with different weights, we obtain a set of linear ordinary first-order differential equations for the moments $\langle \omega^k v^m \rangle$, $k+m=n \in N$. It is evident that the solutions to this equation set are exponents; in particular,

$$\left\langle \omega^n(t) \right\rangle \propto \mathrm{e}^{\lambda_n t}.$$

Substituting this into the set of equations, one obtains an algebraic equation for λ_n. Since we are interested in large values of t, we must choose the largest root for each n. It appears that $\lambda_n(n)$ is a concave function, which means that the statistical moments of vorticity demonstrate intermittent behavior: $\langle \omega^{n+m} \rangle > \langle \omega^n \rangle \langle \omega^m \rangle$.

To understand the mechanism that provides these intermittent correlators, and also in order to extend the results to the cases of finite correlation time or non-Gaussianity, it is useful to develop a mathematical tool for calculating λ_n analytically. It appears that the WKB method is a tool that works very well in the simple case, and can work under weaker assumptions. To simplify the notation, we hereafter write $p(t)$ instead of $p_2(t)$. The probability density $P[p](t)$ is Gaussian, and any average can be written in terms of a continual integral; in particular,

$$\langle \omega^k(t) \rangle = \int \prod_\tau \mathrm{d}p(\tau) P[\rho](t) \omega^k(t)$$

$$= \int \prod_\tau \mathrm{d}p(\tau) \mathrm{e}^{-\frac{1}{2}\int_0^t p^2(t')\mathrm{d}t'} \omega^k[t, p(\tau)].$$

Suppose that a major contribution to the integral is made by the trajectories where p is very large. (We will prove it later on.) The WKB method, up to pre-exponent accuracy, gives for (6) an approximate solution $|\boldsymbol{\omega}(t)| \sim \mathrm{e}^{\int \mathrm{d}t' \sqrt{p(t')}}$. Thus, we obtain

$$\langle \omega^k(t) \rangle \sim \int \prod_\tau \mathrm{d}p(\tau) \mathrm{e}^{\int_0^t \left(-\rho^2/2 + k\sqrt{p}\right)\mathrm{d}t'}.$$

We use the method of saddle points to calculate this integral. The saddle-point trajectory $p_*(t)$ is the one that gives the maximal exponent. Taking the variational derivative with respect to $p(\tau)$, we obtain $-p_*(t) + \frac{k}{2} p_*^{-1/2}(t) = 0$, hence $p_*(t,k) = (k/2)^{2/3}$. We see that the realizations with large and nearly constant $p(t,k)$ give the main contribution to $\langle \omega^k \rangle$. This justifies our supposition made in the beginning of the derivation. Substituting $p_*(t)$, we obtain $\langle \omega^k(t) \rangle \sim \exp\left\{ \frac{3}{2} \left(\frac{k}{2}\right)^{4/3} t \right\}$. Thus,

$$\lambda_k \propto k^{4/3}.$$

Although this result is obtained as an approximation at large values of k, it works very well also for small values. The asymptote is close to the exact values beginning with $k = 2$ (discrepancy ~ 0.1 for $k = 2$). One can show that the results are also valid if δ correlation of $p(t)$ is not assumed [14].

In [15], we also derived the equation for the PDF $f(\omega, \nu)$ for the cylindrical model. We found the asymptote for the integral $P(\omega) = \int f(\omega, \nu)\mathrm{d}\nu$ at large ω:

$$P(\omega) = C\omega^{-4} + \cdots. \tag{7}$$

An analogous expression with the same dependence on ω was obtained in [9] for the general 3D case.

3.3. Gaussianity and negative p

We have already mentioned that in the cylindrical model, there is a restriction demanding that $a(t)$ must be finite. This means that $p(t)$ cannot be Gaussian and delta-correlated. However, this apparent contradiction does not spoil the model. Actually, we can see from the analysis that, under the assumption of Gaussianity and δ correlation (and also for finite correlation time), a major contribution to the correlators is made by the realization of the random process $p(t)$ such that p is positive and nearly constant. The corresponding solution for $\omega(t)$ is a growing exponent. The distortions of the statistics of $p(t)$ caused by the restriction of a finite a concern only the region of negative values p and small ω. So, these corrections would not change the results.

On the other hand, in the general 3D case there are no such restrictions for variables analogous to p, and the assumption of Gaussianity (or at least symmetry) of its PDF is natural. Thus the cylindrical model reflects correctly the statistical properties at large vorticities: for vorticities close to zero, the model is much less confident.

One more comment concerns the requirement of constant sign of vorticity along a trajectory. In the 3D case the corresponding tensor equation requires no such restrictions, and any projection of vorticity may oscillate. However, the absolute value of vorticity would on average grow exponentially, even though p is Gaussian and oscillating regimes for every projection alternate with exponentially growing/decreasing regions.

4. Velocity structure functions

We now discuss the application of the cylindrical model to the calculation of velocity structure functions. We will be interested in longitudinal and transverse structure functions; these are

$$S_n^{\parallel}(l) = \left\langle \left| \mathbf{v}(\mathbf{r}+\mathbf{l}) - \mathbf{v}(\mathbf{r}) \cdot \frac{\mathbf{l}}{l} \right|^n \right\rangle,$$

$$S_n^{\perp}(l) = \left\langle \left| \mathbf{v}(\mathbf{r}+\mathbf{l}) - \mathbf{v}(\mathbf{r}) \times \frac{\mathbf{l}}{l} \right|^n \right\rangle,$$

respectively. The average is taken over all pairs of points separated by a given l. Within the inertial range of scales, the functions demonstrate the scaling behavior

$$S_n^{\parallel}(l) \propto l^{\zeta_n^{\parallel}}, \quad S_n^{\perp}(l) \propto l^{\zeta_n^{\perp}}.$$

The scaling exponents $\zeta_n^{\parallel}$ and $\zeta_n^{\perp}$ are proved to coincide in isotropic flows for $n = 2$ and 3. For other n, the question of whether they coincide or not is open. Many recent experiments and DNS show a difference between $\zeta_n^{\parallel}$ and $\zeta_n^{\perp}$ for larger n, and this is to be understood theoretically.

The cylindrical model is not isotropic. However, isotropy can be obtained if we combine many cylindrical 'bunches' with different orientations.

In [15, 16], we proposed a combination of the VF model with the MF framework. This allowed us to calculate both kinds of scaling exponents. Our assumption is that a major contribution to structure functions (and to intermittent statistics in general) is made by the same high-vorticity VFs that contribute most to vorticity moments. For these filaments, the statistical moments of vorticity and the extremal behavior of the vorticity PDF as $\omega \to \infty$ are known both in the cylindrical model and in the general 3D case [9, 10, 14]. However, it is difficult to relate the statistical characteristics of vorticity to those of velocity. The MF framework provides the means of reaching this goal.

Here we recall briefly the results (which are suited to both the general 3D case and the cylindrical example) and concentrate on the properties of extreme filaments that contribute to the largest-order structure functions.

4.1. Difference between the transverse and longitudinal structure functions: the simplest case

Consider now the simplest case of an axially symmetric filament. In this case, $\mathbf{u} = \boldsymbol{\rho} \times \boldsymbol{\omega}$. In the exponentially growing filament, $b = -2s = \dot{\omega}/\omega \ll \omega$; thus, $\mathbf{u}$ forms a major part of the whole velocity and should make a major contribution to structure functions. However, it does not contribute to the longitudinal structure functions:

$$\Delta v_{\parallel} = (\mathbf{v}\,(\mathbf{r}+\mathbf{l}) - \mathbf{v}(\mathbf{r})) \cdot \mathbf{l}/l \simeq (al_{\perp}^2 + bl_z^2)/l \sim al.$$

In contrast,

$$\Delta v_{\perp} = |(\mathbf{v}\,(\mathbf{r}+\mathbf{l}) - \mathbf{v}(\mathbf{r})) \times \mathbf{l}/l| \simeq \omega l_{\perp} l_z/l \sim \omega l.$$

We find that $\Delta v_{\perp} \gg \Delta v_{\parallel}$; in this simple example, there is no equivalence between longitudinal and transverse structure functions. Considering a set of such filaments with randomly oriented axes restores the isotropy of the flow but does not change the relation between the structure functions. However, adding some asymmetry to each filament would restore the equality.

In our opinion, this may be a clue to understand better the difference observed between longitudinal and transverse velocity scaling exponents.

4.2. MF conjecture

We now recall briefly the main points of the MF model [7, 8]. The model generalizes the Kolmogorov theory (K41) to describe the observed nonlinear dependence of scaling exponents on their order.

The assumption of the model is that a main contribution to velocity structure functions is made by the solutions where

$$\delta v(l) = |\mathbf{v}\,(\mathbf{r}+\mathbf{l}) - \mathbf{v}(\mathbf{r})| \sim l^{h(\mathbf{r})}.$$

So, to calculate structure functions, it is enough to consider only a set of scaling solutions that can be numbered by h. This property is called local scale invariance.

The behavior of correlations at $l \to 0$ is deliberately determined by rare events (otherwise they would be trivial and much smaller, $\langle \Delta v^n \rangle \sim l^n$). From the large fluctuations theorem it follows that the probability of the measured velocity difference $\Delta v(l)$ to have the scaling h is a power-law function of l: $p = l^{3-D(h)}$. Knowing $D(h)$, one could in principle calculate all structure functions:

$$\langle \Delta v^n \rangle = \int l^{nh} l^{3-D(h)} \mathrm{d}\mu(h).$$

Here $\mathrm{d}\mu(h)$ is the measure that is responsible for the relative weights of different values of h. It makes a pre-exponential factor which could give logarithmic corrections to scaling laws. In the limit $l \to 0$, only the smallest exponent contributes to the integral; using the steepest descent method, we obtain

$$\lim_{l\to 0} \frac{\ln\langle \Delta v^n \rangle(l)}{\ln l} = \zeta_n, \quad \zeta_n = \min_h (nh + 3 - D(h)). \tag{8}$$

$D(h)$ is a concave function reaching its maximum at some h_0; according to (8), the requirement $\zeta_0 = 0$ leads to $D(h_0) = 3$.

4.3. Combination with the VF model

The regions of high vorticity are VFs, so they determine the vorticity PDF at large ω. Making use of the ergodic theorem, we write the probability density of vorticity as the spatial average over all filaments:

$$P(\omega) = \frac{1}{V} \int \mathrm{d}\mathbf{r} \delta(\omega - \Omega(\mathbf{r})) = \frac{1}{V} \sum_i \int_{V_i} \mathrm{d}\mathbf{r} \delta(\omega - \Omega_i(\mathbf{r})).$$

Here V is the entire volume of the liquid, the sum is taken over all filaments, and V_i is the volume occupied by the ith filament; $\Omega_i(\mathbf{r})$ is the spatial distribution of vorticity inside the ith filament.

The VFs are strongly elongated, and locally, most of them can be thought of as those in the cylindrical example. Taking, for simplicity, an axially symmetric cylindrical filament with vorticity directed along the z-axis, we obtain

$$P(\omega) = \frac{2\pi L}{V} \sum_i \int \mathrm{d}r\, r\, \delta(\omega - \Omega_i(r)) = \frac{2\pi L}{V} \sum_i \frac{r_i(\omega)}{|\Omega_i{}'_r|}.$$

Here the derivatives are taken at the values of r where vorticity is equal to ω. Multiplying both parts by ω^4 and making use of (7), we obtain

$$\sum_i \frac{r_i(\omega)\omega^4}{|\Omega_i{}'_r(\omega)|} = \text{const}.$$

The VFs are supposed to be the regions responsible for the scaling behavior. Different filaments can have different scaling, so they belong to different 'MF classes' h and make the most important part of each h-class. Thus, we rewrite the sum as an integral over all classes h:

$$\int l^{3-D(h)} \mathrm{d}\mu(h) \frac{r\Omega^4}{|\Omega'_r|} = \text{const}.$$

We now account for the scaling properties inside a fractal. At the given scale l, the major contribution to Δv from a given filament comes from $r \sim l$. Taking account of scaling properties inside a fractal and taking the average over radius l; we obtain $\Omega \sim \Delta v(l)/l \sim l^{h-1}$, $\Omega'_r \sim l^{h-2}$, $r \sim l$. Then

$$\int l^{3-D(h)+3h-1} \mathrm{d}\mu(h) = 1.$$

As $l \to 0$, with the WKB accuracy the integral is equal to $l^{\min_h(3h+2-D(h))}$. The right-hand side does not depend on l, hence

$$\min_h (3h + 2 - D(h)) = 0. \tag{9}$$

Comparing this with (8), we find that the condition is just equivalent to

$$\zeta_3 = 1. \tag{10}$$

Thus, we obtain the well-known exact statement of Kolmogorov's theory just from the MF theory, adding the ideas of cylindrical filament and the stationary vorticity distribution function, without any assumptions on $D(h)$.

4.4. Extreme filament

The range of possible h is restricted by some $h_{\min}$. From the condition [8] $\zeta_n'' < 0$ and from the absence of singularities of Δv at $l \to 0$, it follows that $(\zeta_n)'_n \geqslant 0$ for any n; hence $h_{\min} \geqslant 0$.

In terms of ζ_n, $h = h_{\min}$ corresponds to the limit $n \to \infty$. This limit, in turn, corresponds to very rare events with extremely large values $\Delta v_{(n)} \simeq \langle \Delta v^n \rangle^{1/n}$. To give an estimate of these rare events, we note that

$$\langle \Delta v^n \rangle^{1/n} \propto l^{\zeta_n/n} \to_{n\to\infty} l^{h_{\min}}.$$

A stronger constraint for $h_{\min}$ could appear if the Euler equation would not allow singular behavior of Δv at extremely small l, like $\Delta v(l) \sim l^\alpha$, $\alpha > 0$. Actually, the steeper the $\Delta v(l)$ for a given vortex, the lower the h to which it contributes. The Euler equation gives no limitations for the slope $\Delta v(l)$, so no positive h can be picked as the lower limit. To make sure of that, we consider the extreme filament that corresponds to $h = h_{\min} = 0$.

The value $h_{\min} = 0$ is possible if there exists a filament with $\Delta v \sim l^0$ at very small l. This condition is satisfied if we take in our cylindrical model a filament ('cell') with

$$\mathbf{u} = \mathbf{e}_\phi \cdot c(t). \tag{11}$$

To satisfy (4), the function $c(t)$ has to be $c(t) \propto \exp\{-\int \frac{a(t)}{R} \mathrm{d}t\}$. One can check that in this extreme case, indeed, $\delta v(l) \sim l^0$. The pressure diverges logarithmically; this means that for any positive h, there exists a corresponding velocity distribution with converging pressure.

Thus, in the cylindrical model of stretching filaments we have vortices that correspond to all possible values of h, up to the extremal value

$$h_{\min} = 0. \tag{12}$$

The behavior of $D(h)$ in the vicinity of $h_{\min} = 0$ is also determined by very rare events (or very small regions) with highest velocity differences. Which events should we take into account? To clarify the situation, we first calculate the contribution to velocity structure functions made by the 'extreme' cylindrical filament (11). Recalling that $a \ll \omega$ in the cylindrical model, we neglect the 'large-scale' velocities; only **u** is to be taken into account. Then, expanding $\sin\phi$ near its maximum and using the saddle point method to calculate the integral over r, we find that

$$\begin{aligned}\langle|\delta v_\parallel|^n\rangle &= c^n \int_0^{2\pi} \mathrm{d}\phi \int_0^R r\,\mathrm{d}r\,|\sin\phi|^n \left|\frac{r}{\sqrt{r^2+2rl\cos\phi+l^2}} - 1\right|^n \\ &\simeq c^n \int_0^{2\pi} |\sin\phi|^n \mathrm{d}\phi \int_0^R \left(\frac{r}{\sqrt{r^2+l^2}} - 1\right)^n r\,\mathrm{d}r \\ &\simeq 2\sqrt{\frac{2\pi}{n}} c^n \frac{l^2}{en^2} = l^2 O(n^{-5/2}).\end{aligned}$$

For transverse structure functions, using Cartesian coordinates and expanding the integrand in the vicinity of the saddle point $x = -l/2$, we obtain

$$\begin{aligned}\langle|\delta v_\perp|^n\rangle &= c^n \int\int \mathrm{d}x\mathrm{d}y \left|\frac{l+x}{\sqrt{l^2+2lx+y^2}} - \frac{x}{\sqrt{l^2+y^2}}\right|^n \\ &\simeq \frac{2^n}{n} l^2 \ln\frac{R}{l}.\end{aligned}$$

We see that in both cases the extreme cylindrical filament provides the same limit of the scaling exponent $|\zeta_n|_{n\to\infty} = 2$, which corresponds to $D(0) = 1$. This is reasonable to expect since the value $D(h)$ has the meaning of the probability of finding the region corresponding to h inside a sphere of radius l. So, the dimension of the extreme cylindrical filament is unity.

However, the pre-exponents demonstrate different behavior: actually, at large n values the contribution to the longitudinal structure functions is very small, so it is not noticeable compared to contributions from other filaments with larger h. Thus, the extreme cylindric filaments determine the extreme dimension $D_\perp(0) = 1$ and the limit of the scaling exponent for transverse structure functions:

$$D^\perp(0) = 1, \quad \lim_{n\to 0} \zeta_n^\perp = 2, \tag{13}$$

but they do not contribute to the corresponding longitudinal values. The reason is that, as we discussed above, axially symmetric configurations do not produce longitudinal structure functions. So, these functions must be contributed by some other, even more 'rare', extreme configurations with strongly broken axial symmetry. These are strongly curved extreme filaments.

4.5. Extreme filaments for longitudinal structure functions

The cylindrical model fails to describe the extreme filament that would make the most contribution to $\zeta_n^\parallel$: it is impossible to obtain $D'' \ll 1$ in the cylindrical framework. However, the extreme axial filament gives an idea of how other extreme configurations can be found.

In order to correspond to $h = h_{\min} = 0$, the 'strongly curved extreme filament' must also satisfy $\Delta v(l) \sim l^0$. For simplicity, one can set $v_\phi = 0$ in spherical coordinates. Then the non-divergent solution can be written as

$$v_r = \frac{1}{\sin\theta}\frac{\partial}{\partial\theta}(B\sin\theta), \quad v_\theta = -2B. \tag{14}$$

To satisfy the Euler equation, we need

$$\begin{aligned}2B\frac{\partial}{\partial\theta}\left(\frac{1}{\sin\theta}\frac{\partial}{\partial\theta}(B\sin\theta)\right) + 4B^2 &= r\frac{\partial p}{\partial r}, \\ \frac{\partial}{\partial\theta}\left(B^2\right) - 2B^2\cot\theta &= -\frac{\partial p}{\partial\theta}.\end{aligned}$$

Since the left-hand sides are independent of r, we obtain $p = -c_1 \log r + \pi(\theta)$. (As in the case of cylindrical extreme filaments, logarithmic dependence means that $p(r)$ converges for any $h > 0$.) The analysis of the first equation then shows that there are solutions that diverge logarithmically at $\theta = 0$: $B(\theta \to 0) \simeq \theta\sqrt{-\log\theta}$. This corresponds to $\pi(\theta \to 0) \sim \theta^2$ in the second equation.

Since $\Delta v(l) \sim l^0$ and the average includes $r^2\mathrm{d}r$, the solution gives $\langle\Delta v^n\rangle \propto l^3$; thus, $\lim_{n\to\infty} \zeta_n = 3$, which corresponds to

$$D^\parallel(0) = 0. \tag{15}$$

The logarithmic divergence along the axis $\theta = 0$ would also vanish if one allows any weak dependence on r, i.e. $h < 0$. Such filaments could be made by folding up a 'usual' cylindrical filament, so that the kink is point-like. Also the bending may generally be connected with links of different filaments. Although very rare and unimportant at intermediate n, they become more and more important as n increases.

We stress that all possible kinds of filaments may be presented in a flow, and all of them contribute to all the structure functions. But the fraction of the contributions is different for longitudinal and transverse functions, and this causes the difference between $D^\parallel(h)$ and $D^\parallel(h)$. This can be clearly seen for $h \to 0$ ($n \to \infty$): the transverse scaling exponents are dominated by roughly axially symmetric configurations close to the extreme cylindrical filament (11). The strongly curved configurations close to (14), although occupying much less volume and insufficient for $S_n^\perp$, still dominate in $S_n^\parallel$ where the axial configurations count little.

4.6. Calculation of scaling exponents

Knowing $D(0)$ allows us to find an approximation for $D(h)$ and thus for ζ_n, as was done in [16]. Actually, since we consider the function $D(h)$ as not far from its maximum $D(h_0) = 3$, the simplest function to approximate it is a quadratic expression:

$$D(h) = 3 - b(h - h_0)^2, \quad h \geqslant 0. \tag{16}$$

Here b and h_0 are unknown; conditions (9) and (13), (15) allow us to find these parameters for either $D^\perp(h)$ or $D^\parallel(h)$. The corresponding scaling exponents are

$$\zeta_n = nh_0 - n^2/4b, \quad n \leqslant n_* = 2bh_0, \tag{17}$$

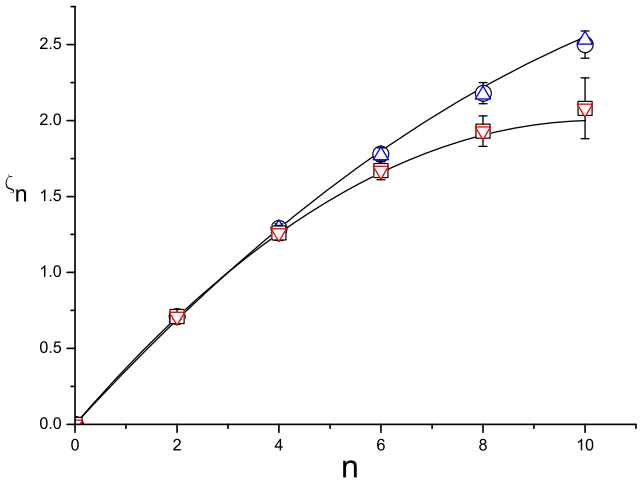

Figure 2. Euler longitudinal (upper branch) and transverse (lower branch) scaling exponents: the results of DNS from [3] (○, □) and [2] (△, ▽) and the result of the theory (17) (lines).

where

$$h_0^{\parallel} \simeq 0.37, \quad b^{\parallel} \simeq 22.3; \quad h_0^{\perp} \simeq 0.39, \quad b^{\perp} \simeq 13.1.$$

In figure 2, we reproduce the resulting graphs $\zeta_n^{\perp}$ and $\zeta_n^{\parallel}$ obtained in [16]. The scaling exponents fit the experimental data very well so that there are no adjusting parameters. A weakness of this result is that whereas it gives $\zeta_3^{\perp} = \zeta_3^{\parallel}$ by construction, it does not satisfy the second exact requirement $\zeta_2^{\perp} = \zeta_2^{\parallel}$. However, the difference is very small: $\zeta_n^{\parallel} - \zeta_n^{\perp} \simeq 10^{-2}$. The equality can be achieved if one takes the third-order terms in $D(h)$ into account. However, the contribution of higher orders to ζ_n at $n \leqslant 10$ would be very small.

For

$$n \geqslant n_* = D'(h_{\min}),$$

the minimum in (8) is reached at the boundary $h = h_{\min}$. From (8) it follows that $\zeta_n|_{n>n_*} = nh_{\min} + 3 - D(h_{\min})$. If $h_{\min}$ were positive, ζ_n would be a linear function; since $h_{\min} = 0$, ζ_n reaches its maximum and becomes constant: $\zeta_n^{\parallel}|_{n>n_*} = 3$, $\zeta_n^{\perp}\big|_{n>n_*} = 2$. The saturation boundary n_* in (17) is $\zeta_n^{\parallel} \simeq 16$, $\zeta_n^{\perp} \simeq 10$. Taking into account the higher-order terms in (16) can shift the value of n_* significantly. Also they would smooth the transition to the constant.

5. Conclusion

We have discussed the cylindrical model that is a particular case of the VF model. It treats VFs in a strongly simplified way, making the picture effectively two dimensional. Still the model provides practically the same results for $\zeta_n^{\perp}$ and a significant part of $\zeta_n^{\parallel}$ as the general VF theory. The reason for the coincidence is probably that most of the filaments are strongly stretched and hence roughly cylindrical. The extreme filaments that contribute to $\zeta_n^{\parallel}$ and $\zeta_n^{\perp}$ at large values of n are considered in detail. We thank Professor Ya G Sinai, M Bustamante, Professor H Baumert and Professor A Klimenko for fruitful discussions. We also thank Professor A V Gurevich for his kind interest in our work. This work was partially supported by the RAS Program 'Fundamental Problems of Nonlinear Dynamics'.

References

[1] Boffetta G, Mazzino A and Vulpiani A 2008 *J. Phys. A: Math. Theor.* **41** 363001
[2] Gotoh T, Fukayama D and Nakano T 2002 *Phys. Fluids* **14** 1065
[3] Benzi R *et al* 2010 *J. Fluid. Mech.* **653** 221
Benzi R *et al* 2009 arXiv:0905.0082v1
[4] Arneodo A *et al* 2008 *Phys. Rev. Lett.* **100** 254504
[5] Zhou T and Antonia A R 2000 *J. Fluid Mech.* **406** 81
[6] Shen X and Warhaft Z 2002 *Phys. Fluids* **14** 370
[7] Parisi G and Frisch U 1985 *Turbulence and Predictability in Geophysical Fluid Dynamics: Proc. Int. School of Physics 'E Fermi' (Varenna, Italy, 1983)* (Amsterdam: North-Holland) pp 84–7
[8] Frisch U 1995 *Turbulence. The Legacy of A N Kolmogorov* (Cambridge: Cambridge University Press)
[9] Zybin P K, Sirota A V, Il'in A S and Gurevich V A 2007 *J. Exp. Theor. Phys.* **105** 455
[10] Zybin P K, Sirota A V, Ilyin S A and Gurevich V A 2008 *Phys. Rev. Lett.* **100** 174504
[11] Zybin P K, Sirota A V, Il'in A S and Gurevich V A 2008 *J. Exp. Theor. Phys.* **107** 879
[12] Zybin P K and Sirota A V 2010 *Phys. Rev. Lett.* **104** 154501
[13] Zybin P K, Sirota A V and Ilyin S A 2010 *Phys. Scr.* **T142** 014005
[14] Zybin P K, Sirota A V and Ilyin S A 2010 *Phys. Rev.* E **82** 056324
[15] Zybin P K and Sirota A V 2012 *Phys. Rev.* E **85** 056317
[16] Zybin P K and Sirota A V 2013 *Phys. Rev. Lett.* submitted (arXiv:1204.1465v1)
[17] Ladyzhenskaya A O 1969 *The Mathematical Theory of Viscous Incompressible Flow* (New York: Gordon and Breach)